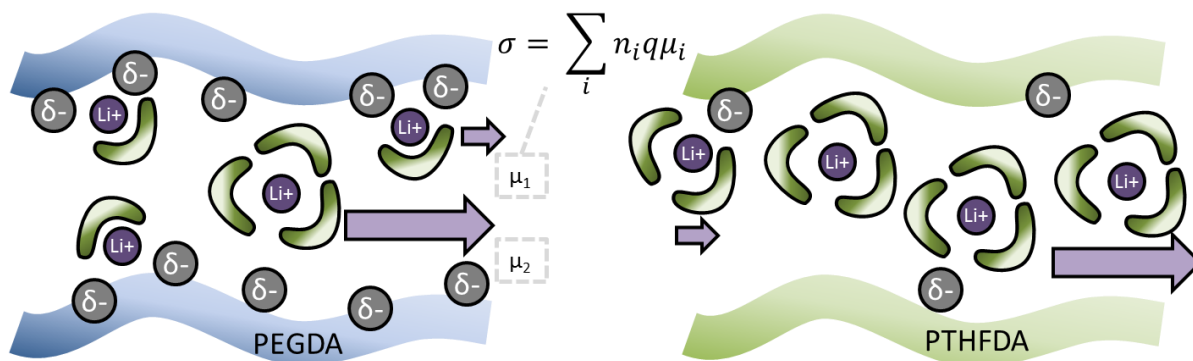


Enhanced Li⁺ conduction within single-ion conducting polymer gel electrolytes via reduced cation-polymer interaction

Hunter O. Ford, Bumjun Park, Jizhou Jiang[†], Jennifer L. Schaefer*

Department of Chemical and Biomolecular Engineering, University of Notre Dame, Notre Dame, IN 46556, USA

ABSTRACT: The development of advanced electrolytes compatible with lithium metal and lithium-ion batteries is crucial for meeting ever growing energy storage demands. One such class of materials, single-ion conducting polymer electrolytes (SIPes), prevents the formation of ion concentration gradients and buildup of anions at the electrode surface, improving performance. One of the ongoing challenges for SIPes is the development of materials that are conductive enough to compete with liquid electrolytes. Presented herein is a class of gel SIPes based on crosslinked poly(tetrahydrofuran) diacrylate that present enhanced room temperature conductivities of 3.5×10^{-5} S/cm when gelled with lithium metal relevant 1,3-dioxolane/dimethoxyethane, 2.5×10^{-4} S/cm with carbonate solutions, and approaching 10^{-3} S/cm with dimethyl sulfoxide. Remarkably, these materials also demonstrate high conductivity at low temperatures, 1.8×10^{-5} S/cm at -20 °C in certain solvents. Most importantly however, when contrasted with identical SIPes formulated with poly(ethylene glycol) diacrylate, the mechanisms responsible for the enhanced conductivity are elucidated: decreasing Li⁺-polymer interactions and gel solvent-polymer interactions leads to an increase in Li⁺ mobility, improving the ionic conductivity. These findings are generalizable to various SIPE chemistries, and can therefore be seen as an additional set of design parameters for developing future high conductivity SIPes.



TOC Image

Introduction

In order to avoid the most catastrophic effects of fossil fuel driven climate change, a widespread shift towards renewable energy sources must be adopted. Of particular interest from the perspective of electrified transportation are so-called “beyond lithium-ion” batteries. Such systems have potential to enable improved battery energy density, life-span, and safety. A major focus of developing beyond lithium-ion batteries is the formulation of an electrolyte that can support these desired characteristics. A common challenge facing liquid and polymer electrolytes that contain dissolved salts is low cation transference numbers, t_+ . In systems where the cation and anion are both freely dissolved in the electrolyte, typically far less than half of the observed conductivity for the electrolyte comes from the motion of the active cationic species.^{1,2} As t_+ approaches unity (i.e. all observed ion conduction is attributed to the active cation), ion concentration gradients in the bulk and anion accumulation at the electrode interface is greatly reduced. Tangible systems benefits of these effects include reduced side reactions, faster rate cycling, and extended cell life span.^{2,3} In an effort to enhance t_+ , a specific class of polymer electrolytes known as single-ion conducting polymer electrolytes (SIPES) has received great attention. SIPES contain covalently anchored anions throughout the polymer. With anchored anions, theoretically all the long-range ion transport observed within such electrolytes can be attributed to the active cationic species, meaning t_+ approaches unity. One of the ongoing challenges however has been designing SIPES that exhibit active ion conductivities on par with conventional liquid electrolytes at room temperature.

State of the art dry SIPES exhibit conductivities on the order of 10^{-6} S/cm with near unity t_+ .⁴⁻⁶ Introduction of solvent into the polymer markedly increases conductivity. Solvent molecules can

plasticize the polymer, enhancing polymer chain segmental motion, increase ion pair dissociation, and offer another transport mechanism for cationic species by facilitating vehicular transport of the solvated cation. Although incorporating solvent into SIPEs increases flammability, relative to conventional liquid electrolytes the overall safety may still be improved.⁷ A number of highly conductive gel SIPEs have recently been demonstrated. Nguyen and colleagues describe a multi-block copolymer with a highly delocalizing tethered anion and partially fluorinated arylene backbone that when swelled in ethylene carbonate (EC) displays a conductivity on the order of 10^{-3} S/cm above 30 °C.⁷ Similarly, Oh and colleagues demonstrated a poly(arylene ether) backbone SIPE with the same order of magnitude conductivity when swelled with carbonate solutions.⁸ Quite recently, Borzutzki and colleagues developed an SIPE with the ionic monomer incorporated within the fluorinated arylene backbone.⁹ This material exhibited a conductivity of 5×10^{-4} S/cm when swelled in a mixture of propylene carbonate (PC) and EC.

Using popular poly(ethylene glycol) (PEG)-based mono and di-functional acrylate monomers along with a delocalizing methacrylate ionic monomer, Porcarelli and coworkers demonstrated a crosslinked network with an impressive 10^{-4} S/cm conductivity when swelled with PC.¹⁰ A similar acrylated PEG network with the ionic monomer 4-styrenesulfonyl (trifluoromethylsulfonyl)imide (STFSI) was demonstrated by Luo and colleagues, displaying a conductivity of 1.8×10^{-4} S/cm at 30 °C when swelled with EC.¹¹

While the progress in SIPE development has been substantial, due to the widely varied polymer chemistries, solvent systems, and testing conditions across the SIPE literature direct comparison of SIPEs in an effort to gain fundamental material insights is limited. With the goal of gaining explicit fundamental understanding that can be used to guide future materials development, we herein present a simple crosslinked SIPE system that allows us to facilely investigate the effect of polymer chain chemistry on ion transport in gel SIPEs. We identify a polymer chemistry that improves lithium ion conduction, and more importantly describe the underlying mechanism responsible for the improvement.

Recently, poly(tetrahydrofuran) (PTHF)-based polymer electrolytes have received renewed attention for their loose cation coordination leading to enhanced conductivity.¹²⁻¹⁴ To our knowledge, we herein present the first SIPE based on PTHF chemistry, and by comparing with a PEG SIPE analog demonstrate the importance of loose Li⁺ coordination in systems that do not contain free salt. We demonstrate that by tuning the polymer chemistry, cation-polymer coordination is reduced and solvent-polymer interactions are altered, enhancing Li⁺ mobility. The former observation is corroborated by recent reports in the literature, while the latter is the first description of the importance of solvent-network interactions for PTHF systems. With this promising polymer chemistry, by screening molecular weight, charge density, and swelling solvent, we demonstrate high conductivity room temperature (25 °C) SIPEs. The best performing materials display lithium conductivities of 3.5×10^{-5} S/cm when swelled with lithium metal relevant ethereal solvents such as 1,3-dioxolane/dimethoxyethane (DOL/DME), 2.5×10^{-4} S/cm with carbonate solutions, and approaching 10^{-3} S/cm with dimethyl sulfoxide (DMSO). Low temperature conductivity is observed to be as high as 1.8×10^{-5} S/cm at -20 °C with select solvents. Furthermore, the self-supported gel SIPEs support limiting currents up to 1.0 mA/cm² at room temperature demonstrating their applicability in beyond lithium-ion batteries. The underlying principles leading to the enhanced Li⁺ conduction in the PTHF-based SIPEs are generalizable to a broad selection of polymer electrolytes, and therefore can be seen as important design characteristics for the engineering of next generation materials.

Polymer synthesis and composition

The SIPE system investigated here is composed of diacrylated crosslinking monomers of varying chemistry and molecular weight copolymerized with STFSI (styrene-SO₂NSO₂CF₃⁻) ionic monomers, the structures of which are shown in Figure S1. The difunctional crosslinkers result in a freestanding SIPE containing anchored ionic units. Two distinct polymer chemistries are explored, poly(ethylene glycol)

diacrylate (PEGDA), and poly(tetrahydrofuran) diacrylate (PTHFDA). PEGDA contains an oxygen and two CH₂ groups per repeat unit (-(OCH₂CH₂)_n-), whereas PTHFDA has an oxygen and four CH₂ groups per repeat unit (-(OCH₂CH₂CH₂CH₂)_n-). By matching the crosslinker molecular weights and charge density, two SIEPs identical in every feature (acrylate content, ionic monomer content, degree of crosslinking, etc.) aside from oxygen density can be directly compared, thus elucidating the impact of polymer chain repeat unit chemistry on ion conduction. Full synthesis protocols for the PTHFDA and STFSI monomers as well as the crosslinked polymers are described in the Supporting Information and in the literature.¹⁵.

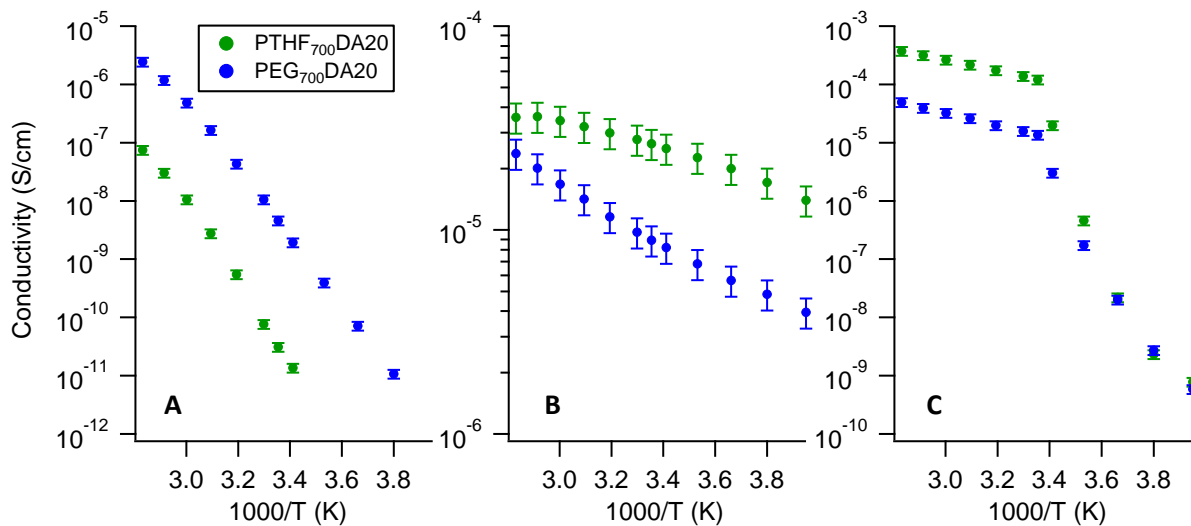


Figure 1. Conductivity of PTHF₇₀₀DA20 and PEG₇₀₀DA20 SIPEs in A. dry state B. DOL/DME swollen state and C. EC/DEC swollen state from -20 °C to 80 °C. Note the approximate melting temperature of the EC/DEC mixture is around 20 °C.

As a starting point, we define our control SIPE as a polymer containing the widely available PEGDA of molecular weight 700 g/mol, with LiSTFSI ionic units at an ether oxygen:charge ratio (EO:Ch) of 20. This system is denoted PEG₇₀₀DA20. For comparison, an SIPE containing PTHFDA of nominal molecular weight 700 g/mol and the same *charge density* (mole of charge per gram of dry polymer) as PEG₇₀₀DA20 was synthesized and denoted PTHF₇₀₀DA20. Note, the EO:Ch for PTHFDA and PEGDA at matching charge densities is necessarily different due to the different network oxygen contents. All composition denotations, charge densities, and associated EO:Ch are shown in Table S1. Considering Eq 1., where σ is conductivity, n is the number density of ions, q is the charge on an ion, and μ is the ion mobility, matching the charge density and crosslinker molecular weight between SIPEs ensures that to the best of our abilities, any differences in conductivity between the networks arises from the chain chemistry.

$$\sigma = n q \mu \quad \text{Eq 1.}$$

Conductivity comparison of SIPEs

The conductivities of PEG₇₀₀DA20 and PTHF₇₀₀DA20 in the as-synthesized dry state and in the gel states when swollen with a 1:1 mixture of DOL/DME or ethylene carbonate and diethyl carbonate (EC/DEC) are presented in Figure 1. The dry PEG₇₀₀DA20 network is notably more conductive than the PTHF₇₀₀DA20 analog, 4.6×10^{-9} S/cm compared with 3.1×10^{-11} S/cm at 25 °C, as evident from Figure 1A. It is well known from the polymer electrolyte work with poly(ethylene oxide) that the mechanism of ion conduction in these dry systems is dependent on ether oxygen-cation interaction.¹⁶ The cation is coordinated by ether oxygens on the polymer chains, and exchanges between coordination sites occur at a rate dependent on the polymer segmental dynamics. The higher density of oxygens in the PEG₇₀₀DA20 SIPE compared to the PTHF₇₀₀DA20 SIPE in the dry state accounts for the former's higher conductivity; the exchange rate of Li⁺ between the available coordination sites in PEO is more facile than PTHF and the dissociation of Li⁺ from the anion may be increased due to the increase in density and interconnectivity of solvation sites.^{17–19} In Figure 2B and 2C, the conductivity relationship is reversed, where now the gel PTHF₇₀₀DA20 is the more conductive SIPE. In DOL/DME at 25 °C, the PEG₇₀₀DA20 displays $\sigma = 8.9 \times 10^{-6}$ S/cm and PTHF₇₀₀DA20 displays $\sigma = 2.7 \times 10^{-5}$, a 200 % increase in conductivity. In EC/DEC at 25 °C, the PEG₇₀₀DA20 exhibits $\sigma = 1.4 \times 10^{-5}$ S/cm and PTHF₇₀₀DA20 exhibits $\sigma = 1.2 \times 10^{-4}$, a 760 % increase in conductivity.

Enhanced ion transport – interactions between cation, polymer, and solvent

The difference in conductivity between the gel SIPEs is a result of differing interactions between lithium cations, solvent molecules, and polymer chains. Within the gel SIPE, a lithium cation can have its coordination sites filled by either solvent molecules, bound anion functionality, or polymer chain segments. Different cation coordination states (coordinated purely by solvent, polymer, or a combination) give rise to different ion mobilities. Ions that are purely solvent coordinated have a greater mobility than those that are coordinated with oxygens on the polymer chain, as the chain dynamics are slower than the

vehicular motion of the small molecule solvated cation.²⁰ A cartoon representation of this proposed phenomenon can be seen in the TOC image. Considering Eq. 2, the observed conductivity is therefore sum of the number density of ions existing in the different coordination states.

$$\sigma = \sum_i n_i q \mu_i \quad \text{Eq 2.}$$

The distribution of ion coordination states within an SIPE is driven by the likelihood that a solvent molecule will exchange with a polymer chain segment within a lithium coordination site. The likelihood of exchange is a function of the interactions between cations, polymer chains, and solvent molecules. For the sake of discussion, we loosely define a so-called “interaction parameter” that consists of considerations such as dielectric constant, sterics/geometry, and dynamics. For example, the interaction parameter between a lithium cation and a solvent molecule will be generally enhanced as the dielectric constant of the solvent is increased. The same holds true for the lithium-polymer interaction parameter, with the additional caveat that by changing oxygen density and distribution throughout the polymer geometric differences are also introduced, i.e. Li⁺ solvation sites are changed.¹⁷⁻¹⁹ In a system with a strong cation-solvent interaction and a weak cation-polymer interaction, the likelihood of exchange from a solvent coordinated state to polymer coordinated state is low.

The third interaction, between solvent and polymer, is generally less considered but is in fact of importance. In the case of greatly different dielectric constants or molecular geometry between solvent and polymer, the solvent-polymer interaction parameter is decreased. Decreasing the solvent-polymer interaction parameter decreases the probability that a cation coordination exchange will take place, as the two moieties are less likely to come into close enough proximity for the exchange to occur. An extreme example of this phenomenon is the formation of water channels in Nafion; the fluorinated Nafion backbone and water are so dissimilar that there is little interaction between the two.²¹ Decreasing the solvent-polymer interaction therefore results in a greater portion of solvent coordinated

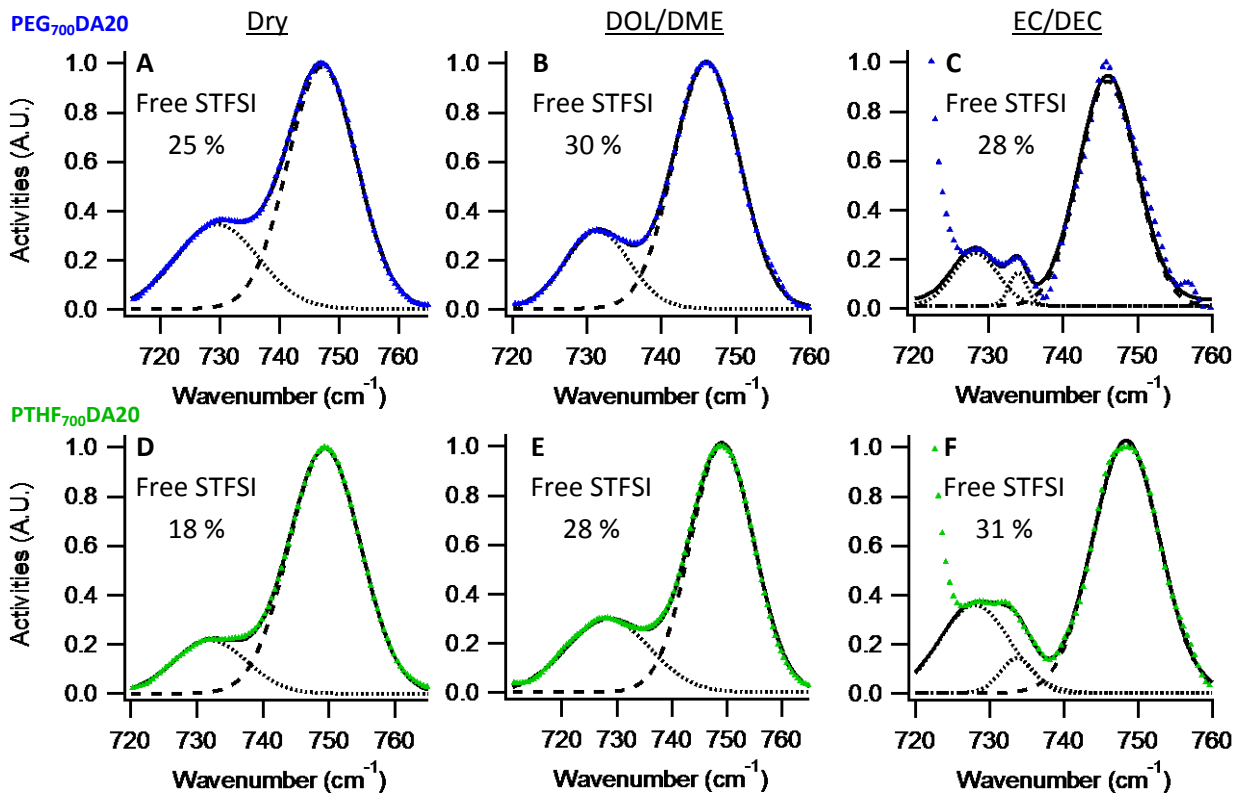


Figure 2. Experimental and fit Raman spectra of $\text{PEG}_{700}\text{DA20}$ and $\text{PTHF}_{700}\text{DA20}$ SIPEs in various swelling conditions.

..... Free STFSI
- - - Associated LiSTFSI
— Combined Fit
▲ Experimental Raman

lithium cations, in that solvent coordinated cations are prevented from interacting with the polymer chain.

The framework of interaction strength fully explains the observed conductivity data. When the solvent-polymer polarity difference is small, such as in the case of the DOL/DME swelled SIPEs, the difference in conductivity is primarily due to the difference in cation-polymer interactions. PTHF has a lower oxygen density and therefore fewer and less interconnected Li^+ coordination sites than PEG. The less lithium interacts with the polymer, the more mobile it is and the greater the conductivity. When the solvent-polymer dielectric difference is large, such as in the case of EC/DEC, there is the additional effect of the decreased solvent-polymer interactions which further ensures the lithium cation remains solvent coordinated. This is why the difference in conductivity between the SIPEs is greater in EC/DEC than DOL/DME, hence the importance of the solvent-polymer interaction cannot be overlooked.

We propose that tuning the cation-polymer and solvent-polymer interaction parameters, accomplished here by decreasing polymer oxygen density, is a useful method for improving Li⁺ conductivity. Up to this point however, only the impact of polymer chemistry on ion mobility has been considered. It is possible that the SIPEs contain a different number of dissociated ionic groups as a result of differing oxygen density. With the use of Raman spectroscopy, the degree of ion dissociation in each SIPE is probed, helping to determine if it is truly a difference in ion mobility or simply a difference in charge carrier density that gives rise to the enhanced PTHF₇₀₀DA20 conductivity.

Raman spectroscopy of SIPEs

The use of Raman spectroscopy is particularly useful for comparing ion dissociation within these SIPEs owing to the strong unique stretch associated with the STFSI anion expansion/contraction.²² We have demonstrated previously with DFT calculations validated with Raman experiments that the stretch associated with the STFSI anion is observed at a different wavenumbers when the anion is associated or dissociated.²³ The dissociated anion stretch is observed around 730 cm⁻¹ and the associated anion stretch is around 748 cm⁻¹. Similar analyses have been performed for liquid and ionic liquid mixtures containing conventional TFSI anions.^{22,24-30} By this method we can compare the STFSI dissociation between PEG₇₀₀DA and PTHF₇₀₀DA SIPEs, gauging the concentration of charge carriers present in each system.

Figure 2 A-F displays experimental and fit Raman spectra for each SIPE in the dry, DOL/DME swollen, and EC/DEC swollen states. The Raman spectra are fit such that peak area comparison provides a quantitative estimate to the percent of dissociated STFSI anions, and therefore percent of Li⁺ not associated with STFSI. In the case of the dry SIPEs, PEG₇₀₀DA20 has a greater degree of STFSI dissociation than PTHF₇₀₀DA20. This is consistent with the conductivity data, and with the notion that in the absence of solvent, network ether oxygens are responsible for dissociating the ionic groups. In the case of the DOL/DME swelled SIPEs, the proportion of dissociated ionic groups is similar between SIPEs, indicating

that in DOL/DME the difference in conductivity does not come from a difference in ion dissociation, and therefore must come from a difference in average ion mobility.

In EC/DEC, the analysis is less straightforward. Firstly, there appear to be three distinct peaks that make up the anion stretch. We attribute the two around 728 cm^{-1} and 735 cm^{-1} to the dissociated anion stretch. Some literature suggests that the lower the wavenumber, the closer the anion is to being fully dissociated.³¹ We tentatively assign the stretch at 728 cm^{-1} to a fully dissociated anion, and the stretch at 735 cm^{-1} to an anion that is in the secondary solvation shell of a Li^+ cation, whereby the anion is dissociated but still influenced by the Li^+ in its local environment. A further complication is the presence of a large peak at 717 cm^{-1} that is due to the EC/DEC solvent, making accurate fitting of the peaks difficult.²⁵ Due to the error in the Raman fitting that comes from the solvent peak interference, the quantitative results should not be over analyzed. Qualitatively, the $\text{PEG}_{700}\text{DA20}$ and $\text{PTHF}_{700}\text{DA20}$ spectra are similar; both contain the two different dissociated anion stretches and the areas corresponding to the total dissociated ions are similar. Accordingly, we believe the difference in conductivity observed in the case of the EC/DEC swollen SIPEs cannot be explained solely by a difference in dissociation degree and must therefore be primarily a function of ion mobility. We conclude that by decreasing the oxygen density within the SIPE network, more of the Li^+ cations are solvent coordinated as opposed to network coordinated, which improves the SIPE conductivity via increased ion mobility.

PTHFDA – Varying molecular weight, charge density, and swelling solvents

With the enhanced conductivity mechanism demonstrated, the molecular weight of the PTHF crosslinker, the charge density of the network, and the swelling solvent were then systematically varied to ascertain the limits of conductivity with PTHF based SIPEs. As can be seen in Figure S2 it was found that conductivity was not altered when molecular weight of the crosslinker was changed, so long as the materials were mechanically similar, further indicating that ion transport in the PTHF based SIPEs is

greatly decoupled from polymer segmental dynamics.²³ To assess the impact of charge density on conductivity, a series of PTHF₇₀₀DA SIPEs with varying charge density (mole of charge per gram of dry polymer) were synthesized. The conductivity of each varying charge density PTHF SIPEs at 25 °C in DOL/DME and EC/DEC is presented in Figure S4 and Figure S5. For EC/DEC the maximum observed was for PTHF₇₀₀DA8, the highest charge density material studied, with $\sigma = 2.5 \times 10^{-4}$ S/cm. For DOL/DME the maximum was observed for PTHF₇₀₀DA12, the second highest charge density material studied, with $\sigma = 3.5 \times 10^{-5}$ S/cm. Refer to Table S1 for exact composition of these samples. PTHF₇₀₀DA12 was chosen as the SIPE for the remaining investigations as it has the highest conductivity in lower dielectric ether based solvents and the second highest conductivity in the higher dielectric carbonate solution.

Besides DOL/DME and EC/DEC, there are many solvents relevant for SIPEs. Higher order glymes such as diglyme and tetraglyme offer increased thermal stability and chelating effects, PC is another common carbonate solution, mixtures of DME and sulfolane have been investigated for use in lithium-sulfur systems, and DMSO is a high dielectric organic solvent.³² Conductivity of PTHF₇₀₀DA12 swelled in each of these solvents is presented in Figure 3. Largely, the results follow expectation. DMSO, known for its solvation strength, yields the highest conductivity due to increased ion dissociation.^{20,33} PC is nearly identical to EC/DEC, with the exception that the PC swollen SIPE maintains an impressive conductivity of 1.8×10^{-5} S/cm even at -20 °C. The ethers likewise follow chemical intuition. As the order of the glyme increases, there is an increase in the chelation strength of the solvent molecule, which can enhance ion dissociation, increasing conductivity. This effect however is offset by an increase in viscosity with order, which decreases ion mobility. Diglyme outperforms DOL/DME, likely due to the chelation effect yet fairly low viscosity of diglyme. Tetraglyme, while having the highest chelation strength, presents a lower conductivity, likely due to the solvent viscosity. The conductivity of the sulfolane/DME mixture is high, even at low temperatures. We have demonstrated previously that as little as 10% by volume of a high dielectric solvent dissolved in a low dielectric solvent yields conductivity on par with that of the pure

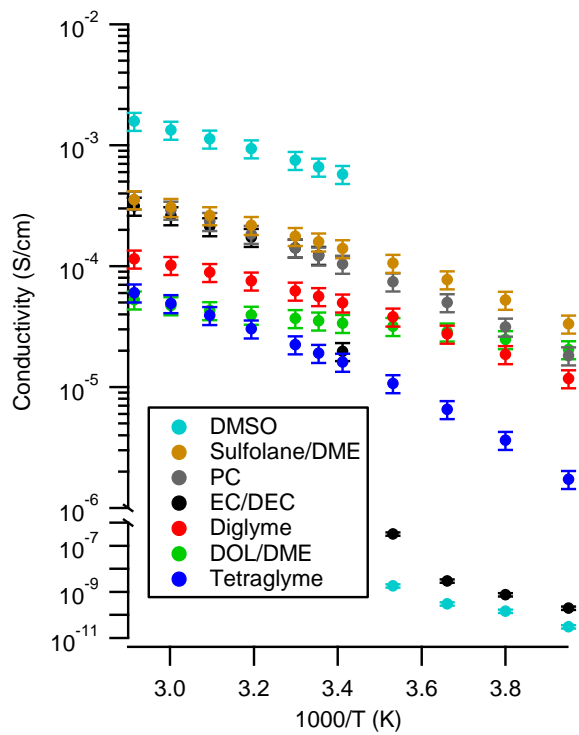


Figure 3. Conductivity of $\text{PTHF}_{700}\text{DA12}$ swelled to equilibrium in a variety of organic solvents. All mixtures are 1:1 by volume.

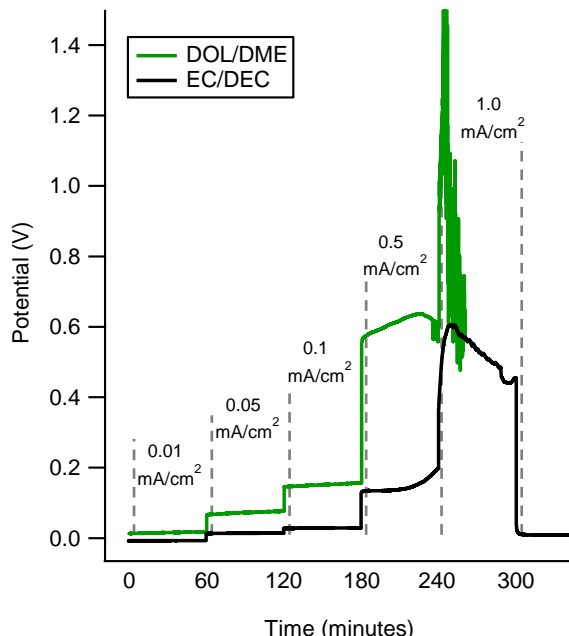


Figure 4. Results of limiting current tests for Li|gel PTHF-based SIPE|Li cells.

high dielectric solvent, which could explain these results.²⁰ Overall, the high conductivity in a variety of solvents demonstrates the versatility of the PTHF based SIPEs.

Application in Lithium cells

Finally, limiting current measurements were performed on Li symmetric cells containing the freestanding $\text{PTHF}_{700}\text{DA12}$ gel electrolytes swelled in DOL/DME or EC/DEC. This was accomplished by application of a galvanostatic current that was sequentially increased after a

period of one hour until cell failure. Despite the chemical incompatibility of EC/DEC with lithium metal, the limiting current supported by the EC/DEC gel was nevertheless examined due to its relevance for Li-ion systems. The results are presented in Figure 4. Self-supported $\text{PTHF}_{700}\text{DA12}$ -based SIPE films enable rates of at least $0.5 \text{ mA}/\text{cm}^2$ in DOL/DME and at least $1.0 \text{ mA}/\text{cm}^2$ in EC/DEC at room temperature. At each current density, the potential of the EC/DEC SIPE is lower than that of the DOL/DME, which should be expected from the conductivity results.

With the use of impedance spectroscopy shown in Figure S6, it was observed that the resistance associated with the bulk polymer electrolyte (165 μm thick) was about

80 Ω and 570 Ω for the EC/DEC and DOL/DME SIPEs, respectively. With the same material but at a thickness of a commercial separator (25 μm) this would translate to a bulk resistance of roughly 12 Ω and 86 Ω , respectively, a significant reduction that would enable even higher rate capabilities.

Conclusions

The impact of polymer chemistry on ion transport within gel SIPEs was characterized. It was found that decreasing the oxygen content within the polymer reduces Li^+ - polymer coordination and modulates how solvent-cation complexes interact with the SIPE, overall improving Li^+ mobility. PTHF based ionic networks, having lower oxygen content than their PEG based analogs, were explored over a variety of crosslinker molecular weights, charge densities, and swelling solvents to better understand PTHF as an SIPE material and probe the limits of achievable conductivity. High room temperature lithium conductivities with lithium metal and lithium-ion relevant solvents were observed, and the best performing PTHF-based gel SIPEs demonstrated relevant limiting currents. These results demonstrate the importance of considering the impact of polymer chain chemistry on ion transport in gels and highlight that slightly tuning relationships that influence transport can have a large impact on performance.

Supporting Information (appended after References)

Experimental procedures, chemical structures, polymer compositions, solvent uptake, molar conductivity data, chain length, charge density and, temperature conductivity data, impedance spectroscopy, scanning electron microscopy, NMR spectroscopy.

Corresponding Author

* E-mail: Jennifer.L.Schaefer.43@nd.edu

Phone: (574)-631-5114

Jennifer L. Schaefer (ORCID): 0000-0003-4293-6328

Present Addresses

†Sichuan University, College of Polymer Science and Engineering, Chengdu, China

Funding Sources

The authors gratefully acknowledge funding from the National Science Foundation via award number CBET-1706370. HOF gratefully acknowledges The Society Of Schmitt Fellows and the Notre Dame CEST Predoctoral Fellowship for additional financial support.

Acknowledgements

The authors thank the Notre Dame Materials Characterization Facility for Raman instrumentation, the Notre Dame Center for Environmental Science and Technology (CEST) for enabling ICP-OES measurements, and the Notre Dame Integrated Imaging Facility for SEM imaging.

REFERENCES

- (1) Zhang, H.; Li, C.; Piszcz, M.; Coya, E.; Rojo, T.; Rodriguez-Martinez, L. M.; Armand, M.; Zhou, Z. Single Lithium-Ion Conducting Solid Polymer Electrolytes: Advances and Perspectives. *Chemical Society Reviews*. **2017**, 797–815.
- (2) Diederichsen, K. M.; McShane, E. J.; McCloskey, B. D. Promising Routes to a High Li⁺ Transference Number Electrolyte for Lithium Ion Batteries. *ACS Energy Lett.* **2017**, 2 (11), 2563–2575.
- (3) Doyle, M.; Fuller, T. F.; Newman, J. The Importance of the Lithium Ion Transference Number in

Lithium/Polymer Cells. *Electrochim. Acta* **1994**, *39* (13), 2073–2081.

- (4) Porcarelli, L.; Shaplov, A. S.; Salsamendi, M.; Nair, J. R.; Vygodskii, Y. S.; Mecerreyes, D.; Gerbaldi, C. Single-Ion Block Copoly(Ionic Liquid)s as Electrolytes for All-Solid State Lithium Batteries. *ACS Appl. Mater. Interfaces* **2016**, *8* (16), 10350–10359.
- (5) Bouchet, R.; Maria, S.; Meziane, R.; Aboulaich, A.; Lienafa, L.; Bonnet, J. P.; Phan, T. N. T.; Bertin, D.; Gigmes, D.; Devaux, D.; et al. Single-Ion BAB Triblock Copolymers as Highly Efficient Electrolytes for Lithium-Metal Batteries. *Nat. Mater.* **2013**, *12* (5), 452–457.
- (6) Devaux, D.; Glé, D.; Phan, T. N. T.; Gigmes, D.; Giroud, E.; Deschamps, M.; Denoyel, R.; Bouchet, R. Optimization of Block Copolymer Electrolytes for Lithium Metal Batteries. *Chem. Mater.* **2015**, *27* (13), 4682–4692.
- (7) Nguyen, H. D.; Kim, G. T.; Shi, J.; Paillard, E.; Judeinstein, P.; Lyonnard, S.; Bresser, D.; Iojoiu, C. Nanostructured Multi-Block Copolymer Single-Ion Conductors for Safer High-Performance Lithium Batteries. *Energy Environ. Sci.* **2018**, *11* (11), 3298–3309.
- (8) Oh, H.; Xu, K.; Yoo, H. D.; Kim, D. S.; Chanthad, C.; Yang, G.; Jin, J.; Ayhan, I. A.; Oh, S. M.; Wang, Q. Poly(Arylene Ether)-Based Single-Ion Conductors for Lithium-Ion Batteries. *Chem. Mater.* **2016**, *28* (1), 188–196.
- (9) Borzutzki, K.; Thienenkamp, J.; Diehl, M.; Winter, M.; Brunklaus, G. Fluorinated Polysulfonamide Based Single Ion Conducting Room Temperature Applicable Gel-Type Polymer Electrolytes for Lithium Ion Batteries. *J. Mater. Chem. A* **2019**, *7* (1), 188–201.
- (10) Porcarelli, L.; Shaplov, A. S.; Bella, F.; Nair, J. R.; Mecerreyes, D.; Gerbaldi, C. Single-Ion Conducting Polymer Electrolytes for Lithium Metal Polymer Batteries That Operate at Ambient Temperature. *ACS Energy Lett.* **2016**, *1* (4), 678–682.

- (11) Luo, G.; Yuan, B.; Guan, T.; Cheng, F.; Zhang, W.; Chen, J. Synthesis of Single Lithium-Ion Conducting Polymer Electrolyte Membrane for Solid-State Lithium Metal Batteries. *ACS Appl. Energy Mater.* **2019**, 2 (5), 3028–3034.
- (12) Wang, J.; Genier, F. S.; Li, H.; Biria, S.; Hosein, I. D. A Solid Polymer Electrolyte from Cross-Linked Polytetrahydrofuran for Calcium Ion Conduction. *ACS Appl. Polym. Mater.* **2019**, 1 (7), 1837–1844.
- (13) Mackanic, D. G.; Michaels, W.; Lee, M.; Feng, D.; Lopez, J.; Qin, J.; Cui, Y.; Bao, Z. Crosslinked Poly(Tetrahydrofuran) as a Loosely Coordinating Polymer Electrolyte. *Adv. Energy Mater.* **2018**, 8 (25), 1800703.
- (14) Du, A.; Zhang, H.; Zhang, Z.; Zhao, J.; Cui, Z.; Zhao, Y.; Dong, S.; Wang, L.; Zhou, X.; Cui, G. A Crosslinked Polytetrahydrofuran-Borate-Based Polymer Electrolyte Enabling Wide-Working-Temperature-Range Rechargeable Magnesium Batteries. *Adv. Mater.* **2019**, 31 (11), 1805930.
- (15) Meziane, R.; Bonnet, J. P.; Courty, M.; Djellab, K.; Armand, M. Single-Ion Polymer Electrolytes Based on a Delocalized Polyanion for Lithium Batteries. In *Electrochimica Acta*; **2011**; Vol. 57, 14–19.
- (16) Xue, Z.; He, D.; Xie, X. Poly(Ethylene Oxide)-Based Electrolytes for Lithium-Ion Batteries. *J. Mater. Chem. A* **2015**, 3 (38), 19218–19253.
- (17) Zheng, Q.; Pesko, D. M.; Savoie, B. M.; Timachova, K.; Hasan, A. L.; Smith, M. C.; Miller, T. F.; Coates, G. W.; Balsara, N. P. Optimizing Ion Transport in Polyether-Based Electrolytes for Lithium Batteries. *Macromolecules* **2018**, 51 (8), 2847–2858.
- (18) Pesko, D. M.; Webb, M. A.; Jung, Y.; Zheng, Q.; Miller, T. F.; Coates, G. W.; Balsara, N. P. Universal Relationship between Conductivity and Solvation-Site Connectivity in Ether-Based Polymer

Electrolytes. *Macromolecules* **2016**, *49* (14), 5244–5255.

- (19) Webb, M. A.; Jung, Y.; Pesko, D. M.; Savoie, B. M.; Yamamoto, U.; Coates, G. W.; Balsara, N. P.; Wang, Z. G.; Miller, T. F. Systematic Computational and Experimental Investigation of Lithium-Ion Transport Mechanisms in Polyester-Based Polymer Electrolytes. *ACS Cent. Sci.* **2015**, *1* (4), 198–205.
- (20) Merrill, L. C.; Ford, H. O.; Schaefer, J. L. Application of Single-Ion Conducting Gel Polymer Electrolytes in Magnesium Batteries. *ACS Appl. Energy Mater.* **2019**, *2* (9), 6355–6363.
- (21) Schmidt-Rohr, K.; Chen, Q. Parallel Cylindrical Water Nanochannels in Nafion Fuel-Cell Membranes. In *Materials for Sustainable Energy*; **2010**; 238–246.
- (22) Herstedt, M.; Smirnov, M.; Johansson, P.; Chami, M.; Grondin, J.; Servant, L.; Lassègues, J. C. Spectroscopic Characterization of the Conformational States of the Bis(Trifluoromethanesulfonyl)Imide Anion (TFSI-). *J. Raman Spectrosc.* **2005**, *36* (8), 762–770.
- (23) Elmore, C. T.; Seidler, M. E.; Ford, H. O.; Merrill, L. C.; Upadhyay, S. P.; Schneider, W. F.; Schaefer, J. L. Ion Transport in Solvent-Free, Crosslinked, Single-Ion Conducting Polymer Electrolytes for Post-Lithium Ion Batteries. *Batteries* **2018**, *4* (2), 28.
- (24) Rey, I.; Lassègues, J. C.; Grondin, J.; Servant, L. Infrared and Raman Study of the PEO-LiTFSI Polymer Electrolyte. *Electrochim. Acta* **1998**, *43* (10–11), 1505–1510.
- (25) McOwen, D. W.; Seo, D. M.; Borodin, O.; Vatamanu, J.; Boyle, P. D.; Henderson, W. A. Concentrated Electrolytes: Decrypting Electrolyte Properties and Reassessing Al Corrosion Mechanisms. *Energy Environ. Sci.* **2014**, *7* (1), 416–426.
- (26) Lassègues, J. C.; Grondin, J.; Aupetit, C.; Johansson, P. Spectroscopic Identification of the Lithium

Ion Transporting Species in LiTFSI-Doped Ionic Liquids. *J. Phys. Chem. A* **2009**, *113* (1), 305–314.

- (27) Fujii, K.; Fujimori, T.; Takamuku, T.; Kanzaki, R.; Umebayashi, Y.; Ishiguro, S. I. Conformational Equilibrium of Bis(Trifluoromethanesulfonyl) Imide Anion of a Room-Temperature Ionic Liquid: Raman Spectroscopic Study and DFT Calculations. *J. Phys. Chem. B* **2006**, *110* (16), 8179–8183.
- (28) Zhou, Q.; Boyle, P. D.; Malpezzi, L.; Mele, A.; Shin, J. H.; Passerini, S.; Henderson, W. A. Phase Behavior of Ionic Liquid-LiX Mixtures: Pyrrolidinium Cations and TFSI- Anions - Linking Structure to Transport Properties. *Chem. Mater.* **2011**, *23* (19), 4331–4337.
- (29) Tchitchevova, D. S.; Monti, D.; Johansson, P.; Bardé, F.; Randon-Vitanova, A.; Palacín, M. R.; Ponrouch, A. On the Reliability of Half-Cell Tests for Monovalent (Li^+ , Na^+) and Divalent (Mg^{2+} , Ca^{2+}) Cation Based Batteries. *J. Electrochem. Soc.* **2017**, *164* (7), A1384–A1392.
- (30) Hardwick, L. J.; Holzapfel, M.; Wokaun, A.; Novák, P. Raman Study of Lithium Coordination in EMI-TFSI Additive Systems as Lithium-Ion Battery Ionic Liquid Electrolytes. *J. Raman Spectrosc.* **2007**, *38* (1), 110–112.
- (31) Suo, L.; Zheng, F.; Hu, Y. S.; Chen, L. FT-Raman Spectroscopy Study of Solvent-in-Salt Electrolytes. *Chinese Phys. B* **2015**, *25* (1), 2014–2017.
- (32) Kolosnitsyn, V. S.; Karaseva, E. V.; Seung, D. Y.; Cho, M. D. Cycling a Sulfur Electrode in Mixed Electrolytes Based on Sulfoblane: Effect of Ethers. *Russ. J. Electrochem.* **2002**, *38* (12), 1314–1318.
- (33) Buss, H. G.; Chan, S. Y.; Lynd, N. A.; McCloskey, B. D. Nonaqueous Polyelectrolyte Solutions as Liquid Electrolytes with High Lithium Ion Transference Number and Conductivity. *ACS Energy Letters*. **2017**, 481–487.

Supplementary Information

Enhanced Li⁺ conduction within single-ion conducting polymer gel electrolytes via reduced cation-polymer interaction

Hunter O. Ford, Bumjun Park, Jizhou Jiang[†], Jennifer L. Schaefer*

Department of Chemical and Biomolecular Engineering, University of Notre Dame, Notre Dame, IN 46556, USA

Experimental

Synthesis of PTHFDA and KSTFSI Monomers

Poly(tetrahydrofuran) (PTHF, Sigma Aldrich) of varying molecular weights (650 g/mol, 1000 g/mol, 2000 g/mol) was dried under dynamic vacuum in an argon filled glovebox (< 10 ppm O₂, < 0.1 ppm water) at 80 °C for 12 hours. After drying, the 650 g/mol and 1000 g/mol PTHF changed from a white semi-liquid material to a clear and colorless liquid. The 2000 g/mol PTHF remained a hard wax after cooling.

In a typical acrylation synthesis where the dihydroxy terminated PTHF monomers are converted to diacrylate terminated, the molar ratio of 1:4:5 PTHF:acryloyl chloride (AC, Sigma Aldrich, 5g ampules): triethylamine (TEA, Sigma Aldrich) was employed. The syntheses were performed on a 10 g scale of AC. All glassware was 120 °C oven dried and throughout this process care was taken to minimize exposure to light. The process was the same for all molecular weights, only changing the amount of PTHF required to keep the above ratio.

Within an argon filled glovebox, previously dried PTHF was dissolved into 100 mL anhydrous dichloromethane (DCM, Sigma Aldrich) in a 500 mL round bottom flask equipped with a large stir bar. To this flask, TEA was added and the solution was stirred. The round bottom flask containing the PTHF/TEA mixture was equipped with an addition flask, which was charged with 30 mL DCM and 10 g AC. The addition funnel was septum capped, and the entire apparatus was removed from the glovebox and attached to a Schlenk line under dry N₂ flow. Under the flow of N₂, the round bottom flask was chilled in an ice-bath for 10 minutes. After cooling, the addition funnel was opened such that the AC solution was dispensed dropwise over a period of about four hours.

After the addition funnel was emptied, the solution was an opaque orange color. It was left covered to stir overnight. The dark orange opaque solution was removed from the Schlenk line and gravity filtered to yield an orange jelly-like solid and a dark brown clear solution. This solution was concentrated to an opaque dark brown residue using rotary evaporation. This residue was added to a large bath of stirred hexane (700 mL) precipitating an orange solid. This mixture was gravity filtered to yield a pale yellow hexane solution and orange solid. The orange solid was stirred overnight in hexane yielding yellow/white precipitate and slight yellow hexane. This process was repeated once more. All hexane layers were combined and the hexane removed with rotary evaporation to yield a slightly yellow clear residue. This was placed under high-vacuum for 24 hours. The lowest molecular weight monomer remained a liquid residue, the 1000 g/mol PTHF was semi-solid, and the 2000 g/mol PTHF solidified into a light yellow wax. Successful synthesis was confirmed with the use of ¹H NMR, shown in Figure S8A,B,C.

The synthesis of potassium 4-styrenesulfonyl (trifluoromethylsulfonyl)imide KSTFSI followed the reported literature procedure.¹

Synthesis of crosslinked SIPEs

The appropriate amount of KSTFSI was dissolved in tetraglyme (TEG, Sigma Aldrich, distilled and stored on molecular sieves within glovebox) with gentle heating. To this solution, diacrylate monomer (PEGDA or PTHFDA) was added and dissolved. PTHFDA solutions, especially those with higher molecular weight PTHFDA, phase separate once dissolved in the TEG/KSTFSI solution. Dichloromethane (DCM) was added which breaks the phase separation resulting in a single phase solution. DCM is added to both PTHFDA and PEGDA containing solutions so that the polymerization conditions are identical. To this monomer solution, 4 wt% with respect to the KSTFSI and crosslinking monomer of photoinitiator 2-hydroxy-4'-(2-hydroxyethoxy)-2-methyl propiophenone (Sigma-Aldrich) was added then dissolved. The monomer solution was sandwiched between two ¼ in. thick borosilicate glass plates (McMaster Carr) separated by 200 um thick glass microscope slides (VWR), which were then placed in a UVC-515 Ultraviolet Multilinker 254 nm UV oven. The plates were flipped every five minutes to ensure both sides of the solution receive equal UV radiation. The monomer solutions were photo-crosslinked for a total of 90 minutes. The resultant polymers were washed with methanol to remove unreacted material. The polymers were then placed in a stirred ion exchange solution of 0.5 M lithium chloride to achieve lithiated forms of the polymer. The ion exchange solvent was methanol for the PTHFDA polymers and 18 MΩ deionized water for the PEGDA based polymers. It was found that the PTHFDA-based ionic polymer does not fully exchange to Li when placed in an aqueous solution, and likewise PEGDA-based ionic polymer does not fully exchange to Li when in a methanol solution. The ion exchange solution was replaced every 12 hours for 48 hours, after which free salt was washed from the films by repeating the same process but with solution that does not contain salt. The films were air dried, brought into an argon filled glovebox, and vacuum dried for 16 hours at 80 °C to remove residual solvent. Ion exchange was confirmed stoichiometric via inductively coupled plasma-optical emission spectroscopy (ICP-OES).

Solvent Drying

All solvents and solvent mixtures used for conductivity measurements were obtained from Sigma Aldrich, and were stored over 3 Å Molecular sieves for at least four days to ensure low moisture content.

Solvent Uptake Measurements

Uniform ¼ in. diameter samples of polymer were prepared and weighed in the dry state, in triplicate. These polymer samples were allowed to swell to equilibrium in the solvent in question (four hours for each sample, which is more than sufficient to reach equilibrium swelling).² The swelled dimensions of the polymer were then measured. Excess solvent was removed from the polymer surface with a Kimwipe tissue, then the solvent mass uptake was measured.

Conductivity Measurements

Dry or swelled polymers were sandwiched between brass electrodes within the glovebox, then conductivity was measured with a Novocontrol Turnkey Broadband Dielectric Spectrometer over the temperature range of -20 °C to 80 °C from cold to hot. The σ_{DC} was extracted as the region over which a plateau in the σ_{AC} vs frequency is observed. The standard error of 16.9 % reported on all conductivity values was calculated by taking the RSD of six measurements on the same polymer composition, representing the error associated with preparing the polymer sample and assembling the conductivity cell. The error reported on molar conductivity values is the 16.9 % RSD error propagated with the error from the swelling measurements for a given polymer composition.

Raman Spectroscopy

Within the glovebox, polymer samples were swelled in the appropriate solvent, then placed against the wall of a quartz cuvette, which was then sealed and parafilmed. The Raman spectra were acquired with a NRS-5100 Raman microscope using a 532 nm excitation laser, 20x magnification lense, 25 x 1000 um

slit dimension and 4000 um aperture from 8 to 1900 cm^{-1} at 0.5 cm^{-1} resolution. Exposure was 60 seconds with 7 accumulations. Peak analysis was applied as reported previously.³

NMR Spectroscopy

NMR spectra of synthesized PTHFDA monomers was acquired using a Bruker AVANCE III HD 400 Nanobay and processed with TopSpin Software. Spectra were collected in CDCl_3 .

Scanning Electron Microscopy (SEM)

$\text{PTHF}_{700}\text{DA12}$ samples were swelled in methanol, dunked in liquid N_2 until frozen, then fractured while still under liquid N_2 to produce a clean break for imaging the cross section. Images were collected on a Magellan 400 Digital Field Emission Scanning Electron Microscope at a potential of 2.00 kV and beam current of 6.3 pA. Samples were sputter coated with 2.0 nm of iridium to avoid charging of the non-conductive polymer.

Lithium Symmetric Cells

Within the glovebox, lithium metal (Alfa Aesar, 0.75 mm thick, 99.9 %) was polished to a reflective shine by removing the oxide layer. Two 3/8 in. diameter lithium disks were prepared from the polished metal. A 5/8 in. diameter sample of the SIPE to be tested was swelled in the appropriate solvent. Within 2032 type coin cells (MTI Corp), the swelled SIPE was placed between the two lithium electrodes in contact with the polished side. With the use of two stainless steel spacers (15.5 mm diameter x 0.2 mm thick) and one wave spring the cell was sealed with an electronic crimper. After resting for one hour, the cells were employed in electrochemical characterization. For the impedance spectroscopy and evaluation of t_{Li^+} , measurements were performed with an Ametek Princeton Applied Research Parstat MC.

For the evaluation of the limiting current, a Neware Battery Systems Battery Tester was used. Increasing galvanostatic currents corresponding to 0.01 mA/cm^2 , 0.05 mA/cm^2 , 0.1 mA/cm^2 , 0.5 mA/cm^2 , etc, with

respect to the lithium anode, were applied for one hour while the potential across the cell was measured. The current was increased until obvious cell failure was observed.

Figures, tables, and further discussion

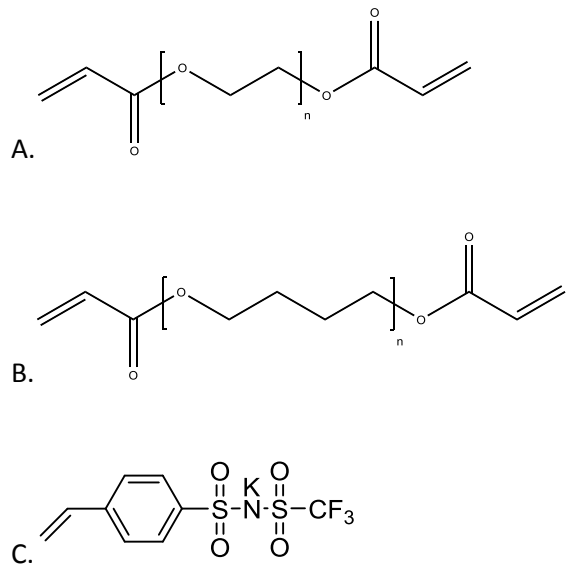


Figure S1. Chemical structures of A. PEGDA, B. PTHFDA, and C. KSTFSI

Table S1. Compositions, formulations, ether oxygen: charge ratio (EO:Ch), and charge density for studied SIEPs.

Sample Name	Crosslinker	Crosslinker mass (g)	KSTFSI (g)	TEG (g)	DCM (g)	EO:Ch	Charge density (mol Ch/g dry polymer)
PEG ₇₀₀ DA20	PEGDA, 700 g/mol	0.300	0.100	0.55	0.288	20	0.00070
PTHF ₇₀₀ DA20	PTHFDA, 700 g/mol	0.300	0.100	0.55	0.288	14	0.00070
PTHF ₁₀₀₀ DA20	PTHFDA, 1000 g/mol	0.300	0.100	0.55	0.288	14	0.00070
PTHF ₂₀₀₀ DA20	PTHFDA, 2000 g/mol	0.300	0.100	0.55	0.288	15	0.00070
PTHF ₇₀₀ DA45	PTHFDA, 700 g/mol	0.350	0.050	0.55	0.288	32	0.00036
PTHF ₇₀₀ DA30	PTHFDA, 700 g/mol	0.330	0.072	0.55	0.288	21	0.00051
PTHF ₇₀₀ DA12	PTHFDA, 700 g/mol	0.259	0.141	0.55	0.288	8	0.00100
PTHF ₇₀₀ DA8	PTHFDA, 700 g/mol	0.220`	0.180	0.55	0.288	6	0.00127

Table S2. Solvent uptake data, by mass and volume, after four hours of swelling for studied SIPEs.

*Calculated by measuring change in thickness and diameter. ** calculated by measuring change in thickness and assuming isotropic expansion.

Sample	Solvent	Mass % increase	Volume % increase
PEG ₇₀₀ DA20	EC/DEC	161.1 ± 10.1	34.9 ± 5.1*
PEG ₇₀₀ DA20	DOL/DME	79.0 ± 5.8	28.2 ± 2.5*
PTHF ₇₀₀ DA20	EC/DEC	157.4 ± 7.6	38.4 ± 2.5*
PTHF ₇₀₀ DA20	DOL/DME	132.9 ± 10.7	40.6 ± 0.2*
PTHF ₁₀₀₀ DA20	EC/DEC	156.1 ± 13.6	38.7 ± 3.6*
PTHF ₁₀₀₀ DA20	DOL/DME	159.0 ± 21.6	40.5 ± 2.1*
PTHF ₂₀₀₀ DA20	DOL/DME	282.9 ± 27.9	57.6 ± 7.6*
PTHF ₇₀₀ DA12	DMSO	-	55**
PTHF ₇₀₀ DA12	Sulfolane/DME	-	27**
PTHF ₇₀₀ DA12	PC	-	27**
PTHF ₇₀₀ DA12	Diglyme	-	32**
PTHF ₇₀₀ DA12	Tetraglyme	-	33**
PTHF ₇₀₀ DA45	EC/DEC	-	22**
PTHF ₇₀₀ DA45	DOL/DME	-	34**
PTHF ₇₀₀ DA30	EC/DEC	-	46**
PTHF ₇₀₀ DA30	DOL/DME	-	39**
PTHF ₇₀₀ DA12	EC/DEC	-	37**
PTHF ₇₀₀ DA12	DOL/DME	-	37**
PTHF ₇₀₀ DA8	EC/DEC	-	48**
PTHF ₇₀₀ DA8	DOL/DME	-	36**

Impact of PTHF crosslinker molecular weight on conductivity

Previously, we have demonstrated that the molecular weight of the crosslinker can impact ion transport within SIPEs. A higher molecular weight crosslinker leads to greater distance between crosslinking junctions and ionic units/aggregates, which in turn leads to an increase of polymer chain segmental motion.⁴ Enhancing the segmental motion improves the mobility of network-coordinated cations. This holds true until the length of the crosslinker is long enough that chains are able to crystallize between crosslinking junctions, a process that decreases segmental motion.^{3,5,6} A series of SIPEs with crosslinking molecular weights of 1000 g/mol and 2000 g/mol were synthesized at the same charge density as PTHF₇₀₀DA20, and denoted PTHF₁₀₀₀DA20 and PTHF₂₀₀₀DA20, respectively. The conductivity of these SIPEs swelled in DOL/DME and EC/DEC is presented in Figure S2. The molar conductivity equivalent is

presented in FIGURE S3. PTHF₇₀₀DA20 and PTHF₁₀₀₀DA20 present near identical conductivity results in both solvent systems. PTHF₂₀₀₀DA20, is slightly lower in DOL/DME than the other chain lengths but the same order of magnitude. It is possible that in the PTHF₂₀₀₀DA20 SIPE, there is enhanced ionic aggregation, as the STFSI/acrylate ratio decreases when the crosslinker length is increased and the charge density is kept the same. Interestingly, PTHF₂₀₀₀DA20 was not mechanically stable when swelled in EC/DEC, precluding its measurement in that solvent. The most likely cause is the decreased mechanical integrity stemming from a decrease in crosslink density. From these results it can be concluded that as long as the network ionic aggregation / crosslinking density is similar, molecular weight does not impact cation transport. This is further evidence that the dissociated Li⁺ cations in PTHF based SIPEs are decoupled from polymer segmental dynamics. The trends are not changed when scaled on the basis of molar conductivity, indicating the trends are independent of the swelling uptake.

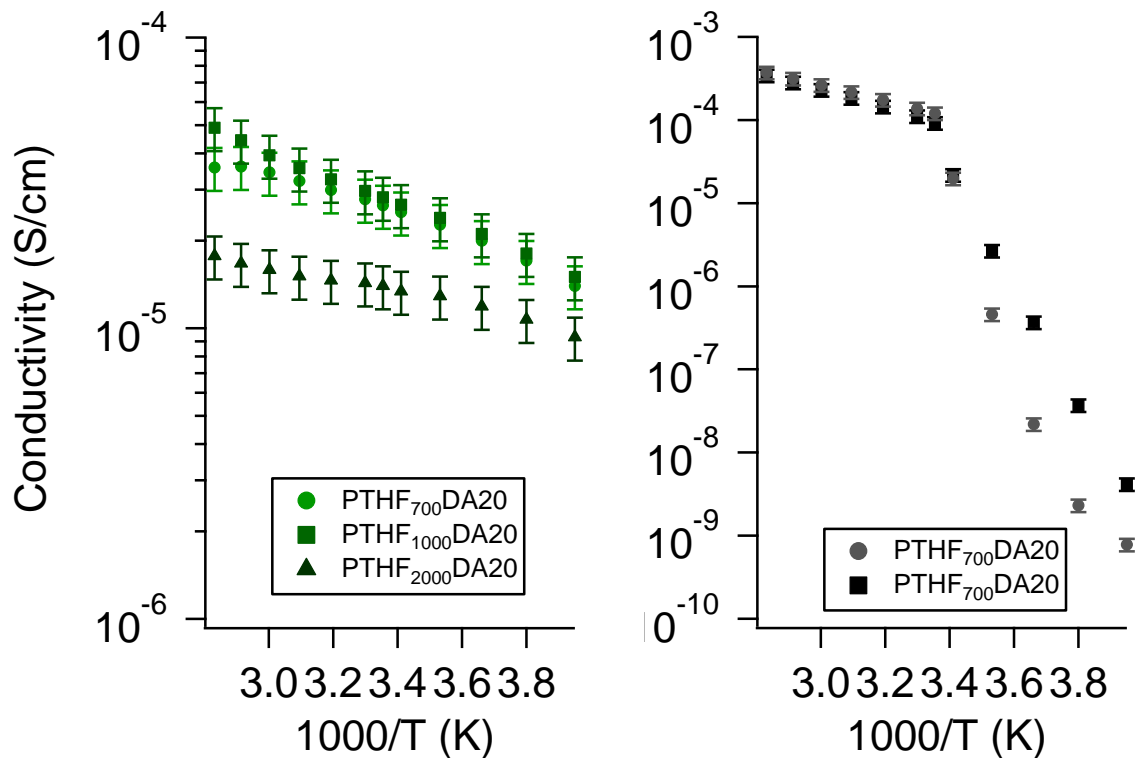


Figure S2. Conductivity of varying crosslinker length PTHF-based SIPEs in DOL/DME (left) and EC/DEC (right)

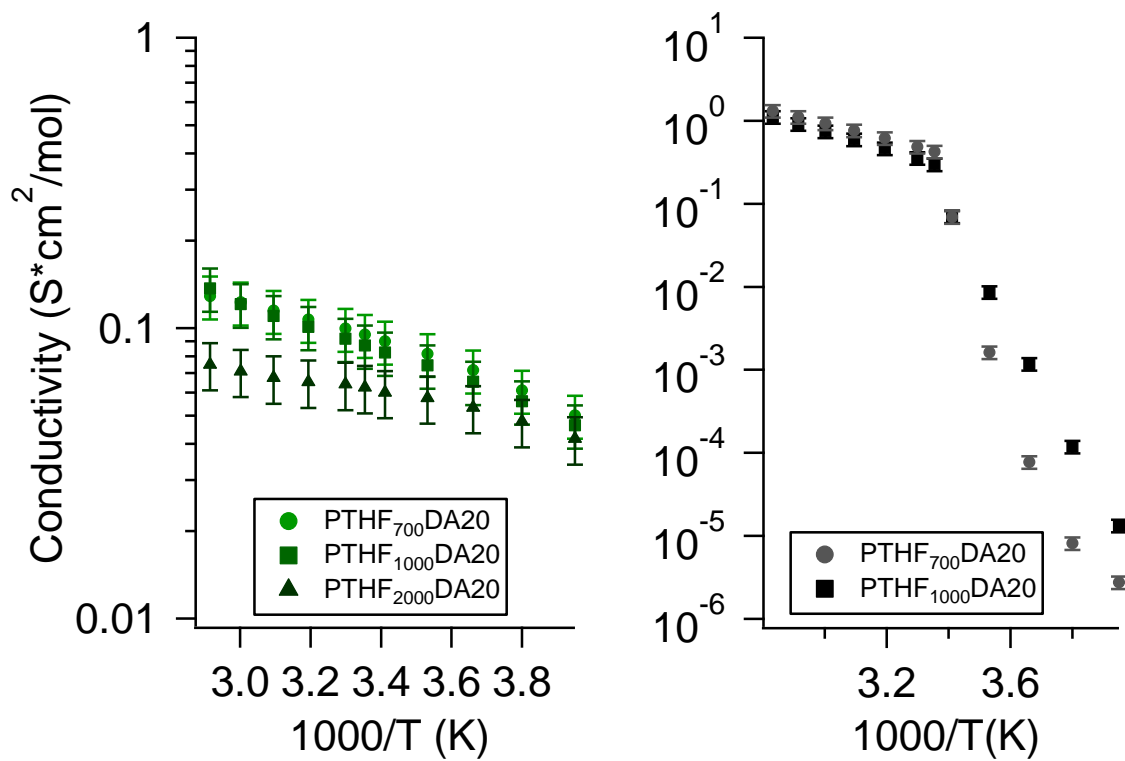


Figure S3. Molar conductivity of varying crosslinker length PTHF-based SIPEs in DOL/DME (left) and EC/DEC (right)

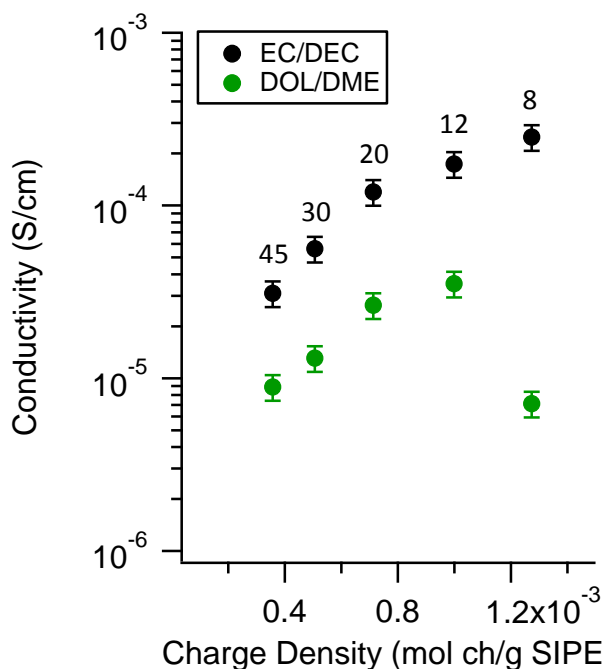


Figure S4. Conductivity of PTHF₇₀₀DA SIPEs swelled in EC/DEC and DOL/DME at 25 °C.

Impact of PTHF SIPE charge density on conductivity

A series of PTHF-based SIPEs with varying charge density (mol of charge per gram of polymer) were synthesized and measured in DOL/DME and EC/DEC. These are denoted PTHF₇₀₀DA8, PTHF₇₀₀DA12, PTHF₇₀₀DA30, and PTHF₇₀₀DA45, where PTHF₇₀₀DA8 has the highest charge density and PTHF₇₀₀DA45 has the lowest. The charge densities were chosen to match the

charge densities of PEGDA-based SIPEs that have an EO:Ch of 8, 12, 30, and 45. Again, note the actual EO:Ch of the PTHF systems are not 8, 12, etc. but the nomenclature is presented this way for clarity. Refer to Table S1 for the true PTHF EO:Ch.

Generally, for these materials there exists a charge density for which a maximum conductivity is observed. Where the maximum is located is a function of the lithium cation solvating ability of the solvent as well as the network chemistry.^{3,7} Most often, as the dielectric constant of the solvent increases, the maximum conductivity value shifts to higher charge densities, as the solvent is capable of dissociating a greater number of ionic units. Figure S5 shows the full temperature dependent conductivity of the varying charge density SIPEs, over which the same trends are observed at every temperature (above the melting point of the solvent mixture).

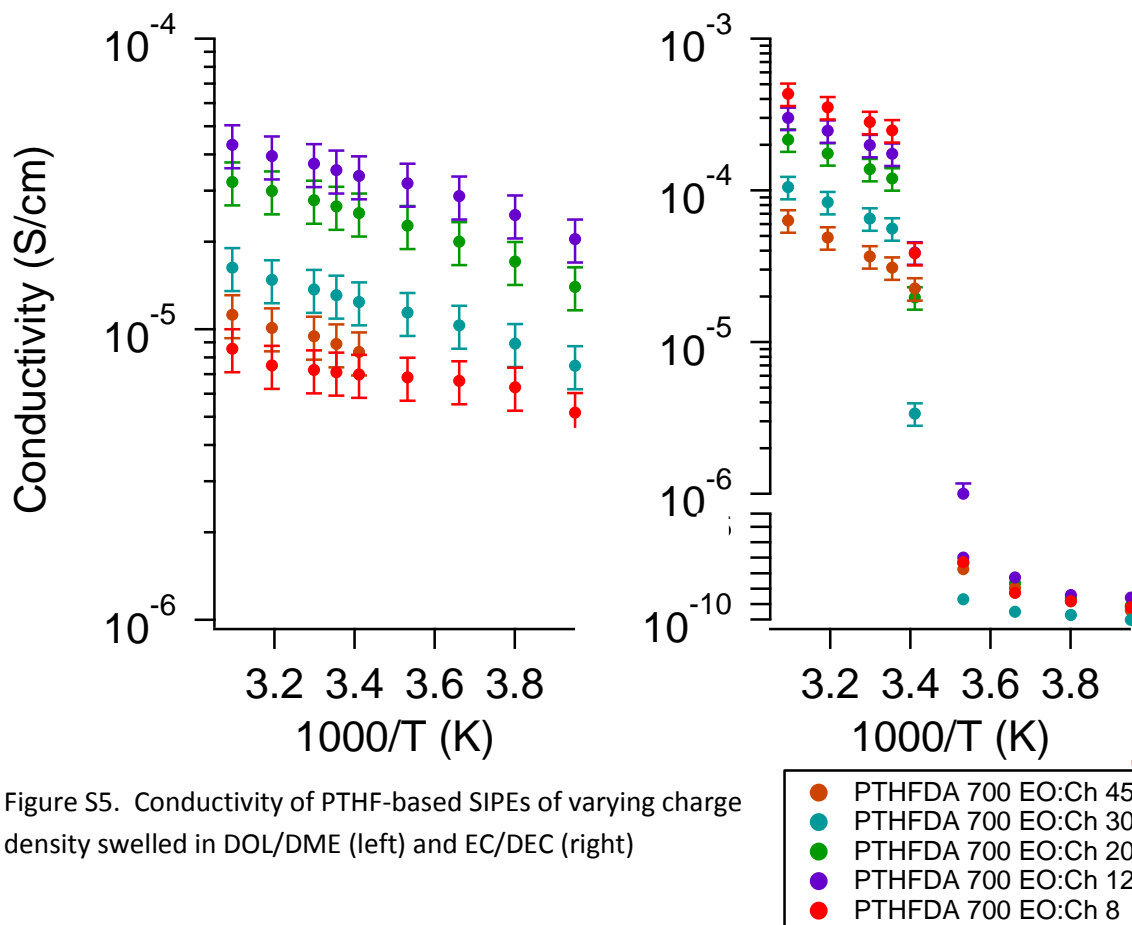


Figure S5. Conductivity of PTHF-based SIPEs of varying charge density swelled in DOL/DME (left) and EC/DEC (right)

Impedance Spectroscopy

t_{Li^+} values for the PTHF₇₀₀DA12 gel electrolyte in DOL/DME and EC/DEC were measured by using the Bruce-Vincent method.⁸ Briefly, a constant potential was applied to a Li|gel electrolyte|Li cell, and the initial current is compared to the steady state current with a correction based on the resistance across the cell according to Eq. S1.

$$t_{Li^+} = \frac{I_{ss}(V - I_o R_o)}{I_o(V - I_{ss} R_{ss})} \quad \text{Eq S1.}$$

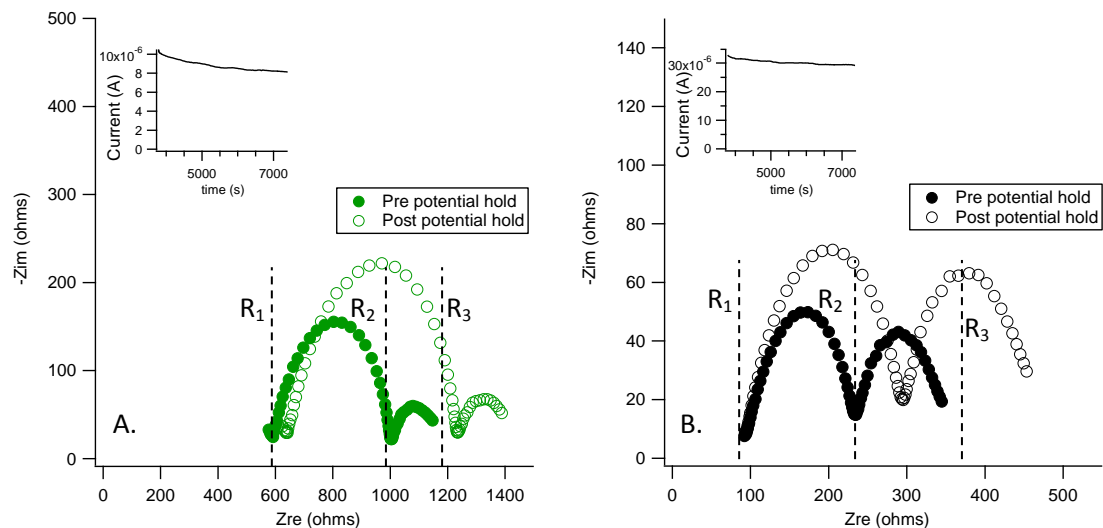


Figure S6. Impedance response pre and post potential hold of Li symmetric cells with A. DOL/DME gel SIPE and B. EC/DEC gel SIPE. Inset shows current response to potential hold.

Where I_o is the initial current, I_{ss} is the steady state current, V is the potential hold, R_o is the initial resistance, and R_{ss} is the steady state cell resistance.

Figure S6A and B show the impedance response before and after the potential hold for the DOL/DME and EC/DEC gel electrolytes, respectively. Firstly, it can be seen there is a greater overall resistance across the DOL/DME cell than the EC/DEC cell, which may be expected from the difference in conductivity of these two electrolytes. In both cases, the total resistance increases after the potential

hold, indicating breakdown of some component of the electrolyte on the lithium metal surface. Each semicircle is fit with a simple binomial to obtain the Z_{re} values when $Z_{im} = 0$. The relevant values obtained are presented in Table S3, and are used along with I_{ss} , I_o , and $V = 11.96$ mV (nominal 10 mV) to calculate t_{Li+} .

Table S3. Extracted resistance and current values from impedance and polarization measurements, respectively, on symmetric lithium cells containing the gel electrolytes.

Sample	R_1 (ohms)	R_3 (ohms)	R_{ss} or R_o (R_1-R_3) (ohms)	I_{ss} (A)	I_o (A)
DOL/DME pre-hold	593	1165	572	-	1.05×10^{-6}
DOL/DME post-hold	640	1421	781	8.25×10^{-5}	-
EC/DEC pre-hold	90	355	265	-	3.38×10^{-5}
EC/DEC post-hold	90	470	380	2.39×10^{-5}	-

For the DOL/DME SIPE, $t_{Li+} = 0.84$, and for the EC/DEC SIPE, $t_{Li+} = 0.66$. It should be mentioned that the exact values of these transference numbers are not to be over-interpreted, and should instead be considered as estimates. In both cases, the values are high relative to the values obtained for free salt liquid electrolytes under similar conditions indicating the truly single-ion conducting nature of these SIPEs.^{9,10} Decomposition of the solvent in contact with lithium metal is expected to lead to the error in the t_{Li+} measurements for gel SIPEs.

The presence of two semicircles in each measurement suggests the cell circuit cannot be modeled by a single R-Q element in addition to the standard bulk resistance. R_1 is assigned as the bulk resistance through the SIPE. R_2 is assigned as the charge transfer resistance, which increases after the potential hold as a result of decomposition on the lithium metal. This leaves the assignment of R_3 . To rule out that there are multiple polymer morphologies that could have different resistances (and therefore

demonstrate a double two R-Q system behavior) scanning electron microscopy (SEM) is used to investigate the cross section of the PTHF₇₀₀DA12 SIPE in the dried state. These images can be seen in Figure S7.

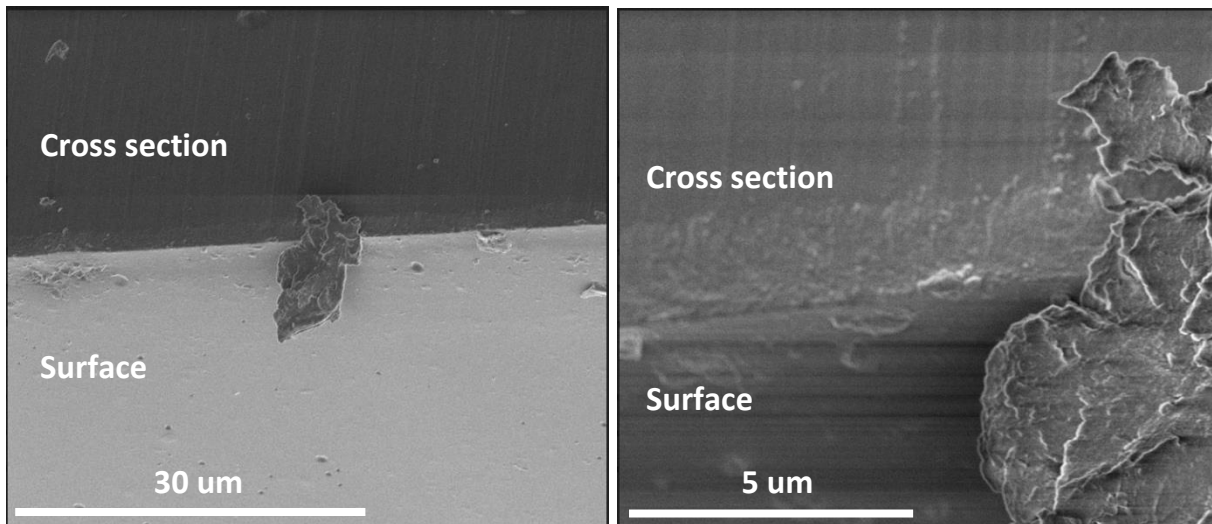


Figure S7. SEM cross section of pristine PTHF₇₀₀DA12 SIPE at different magnifications. Focused on area containing defect for visual context.

As can be seen in Figure S7, it appears as though the cross section and surface present the same morphology, a dense material without permanent pore structure or otherwise remarkable features. This indicates that the second semi-circle does not stem from a polymer inhomogeneity.

Without clear evidence that R_3 is related to bulk polymer material morphology, R_3 is speculatively assigned as the resistance across a small layer that likely exists between the lithium metal and the gel SIPE, a product of a reaction between the lithium metal and the SIPE. This region is effectively an SEI. It has been demonstrated in the literature that under the right conditions, presence of an SEI with appropriate thickness and with transport properties sufficiently different than the bulk electrolyte satisfies the conditions necessary to model the cell as a circuit containing an R-Q component and a

finite-distance Warburg diffusion impedance element.¹¹⁻¹³ We have observed similar behavior in magnesium symmetric cells employing SIPE gels.² This behavior is in contrast to the semi-infinite 45° Warburg element commonly seen in liquid electrolyte impedance data. The difference in applying the semi-infinite as opposed to finite Warburg element stems from the relationship between the length scale of the layer in question and the time scale of the impedance measurement (i.e. from the perspective of the measurement, a microns thick bulk electrolyte would appear semi-infinite while a nanometers thick SEI would appear finite).

This leaves us to maintain the hypothesis that R_3 stems from the resistance across an SEI interlayer between the lithium metal and the SIPE. The absolute identification and characterization of this SEI is beyond the scope of the present investigation, however it is the subject of ongoing future work.

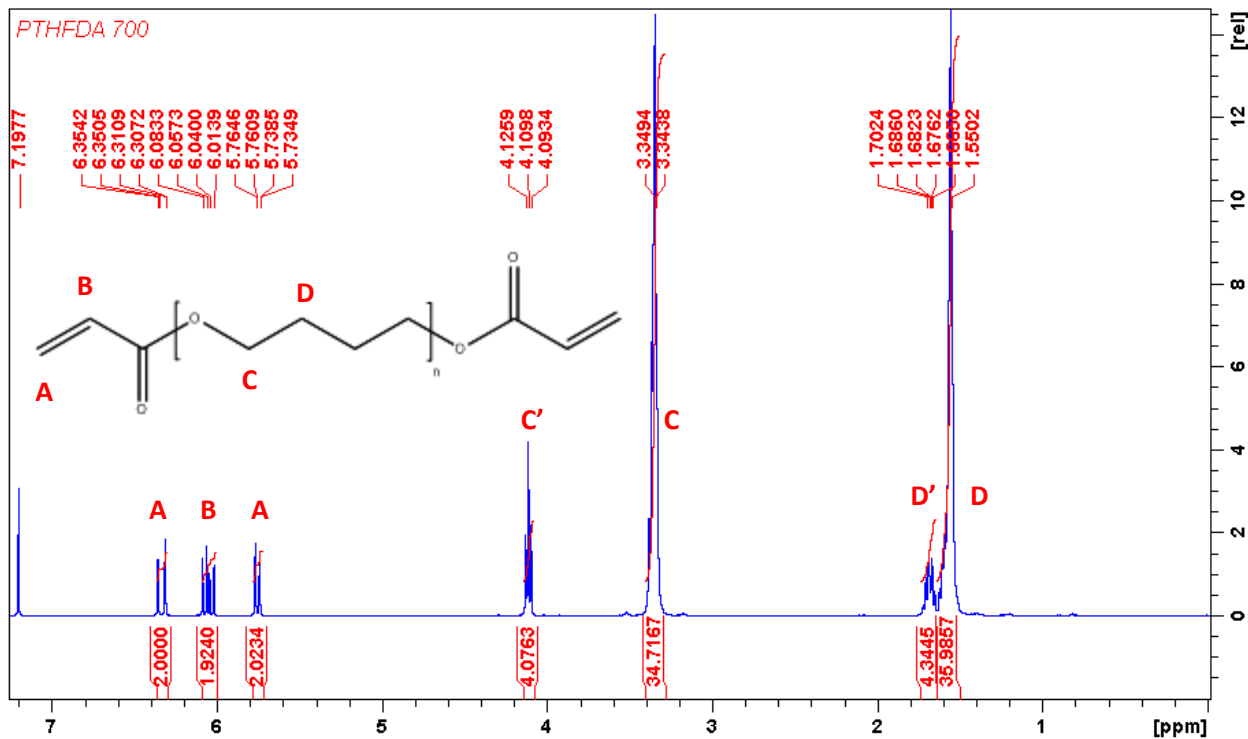


Figure S8A. ¹H NMR for PTHF₇₀₀DA with labeled protons. (CDCl₃, 400 MHz). δ 1.55 (m, 36H, H_D), 1.68 (m, 4H, H_{D'}), 3.34 (m, 35H, H_C), 4.1 (t, 4H, H_{C'}), 5.74 (dd, 2H, H_A), 6.01 (dd, 2H, H_B), 6.31 (dd, 2H, H_A). Integrations are such that the entire molecule is considered, i.e. the aliphatic protons C/D represent all the aliphatic protons on the oligomer, A and B are the vinyl protons on both acrylate groups. C' and D' are the protons on carbons that are on the first repeat unit after the acrylate group, which causes their chemical shift to be increased. By summing the integration of C, C', D, D', the total number of repeat units can be determined. That total is about 80 protons, which corresponds to 10 repeat units. Each repeat unit has a mass of 72 g/mol. With the acrylate groups, total molecular mass is estimated at 846 g/mol.

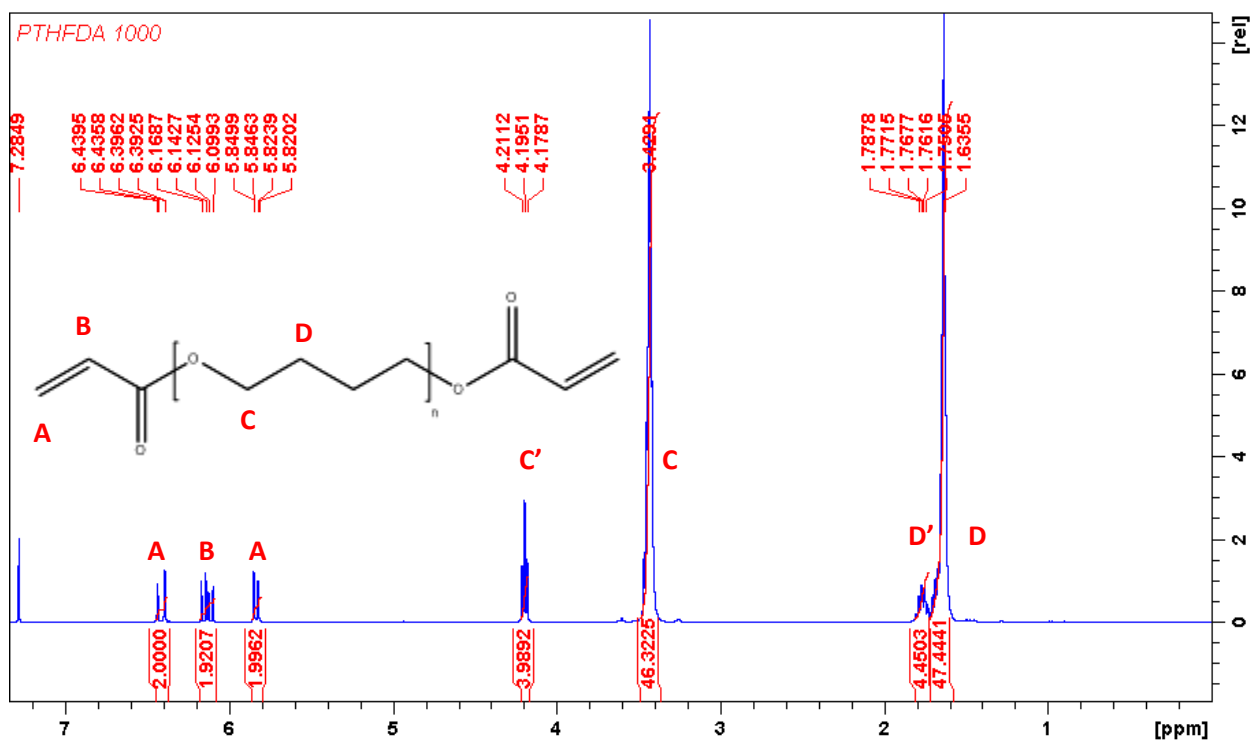


Figure S8B. ^1H NMR for $\text{PTHF}_{1000}\text{DA}$ with labeled protons. (CDCl_3 , 400 MHz). δ 1.63 (m, 48H, H_D), 1.76 (m, 4H, $\text{H}_{D'}$), 3.42 (m, 46H, H_C), 4.19 (t, 4H, $\text{H}_{C'}$), 5.82 (dd, 2H, H_A), 6.09 (dd, 2H, H_B), 6.39 (dd, 2H, H_A). There are about 102 aliphatic protons, which corresponds to 13 repeat units. Each repeat unit has a mass of 72 g/mol. With the acrylate groups, total molecular mass is estimated at 1062 g/mol.

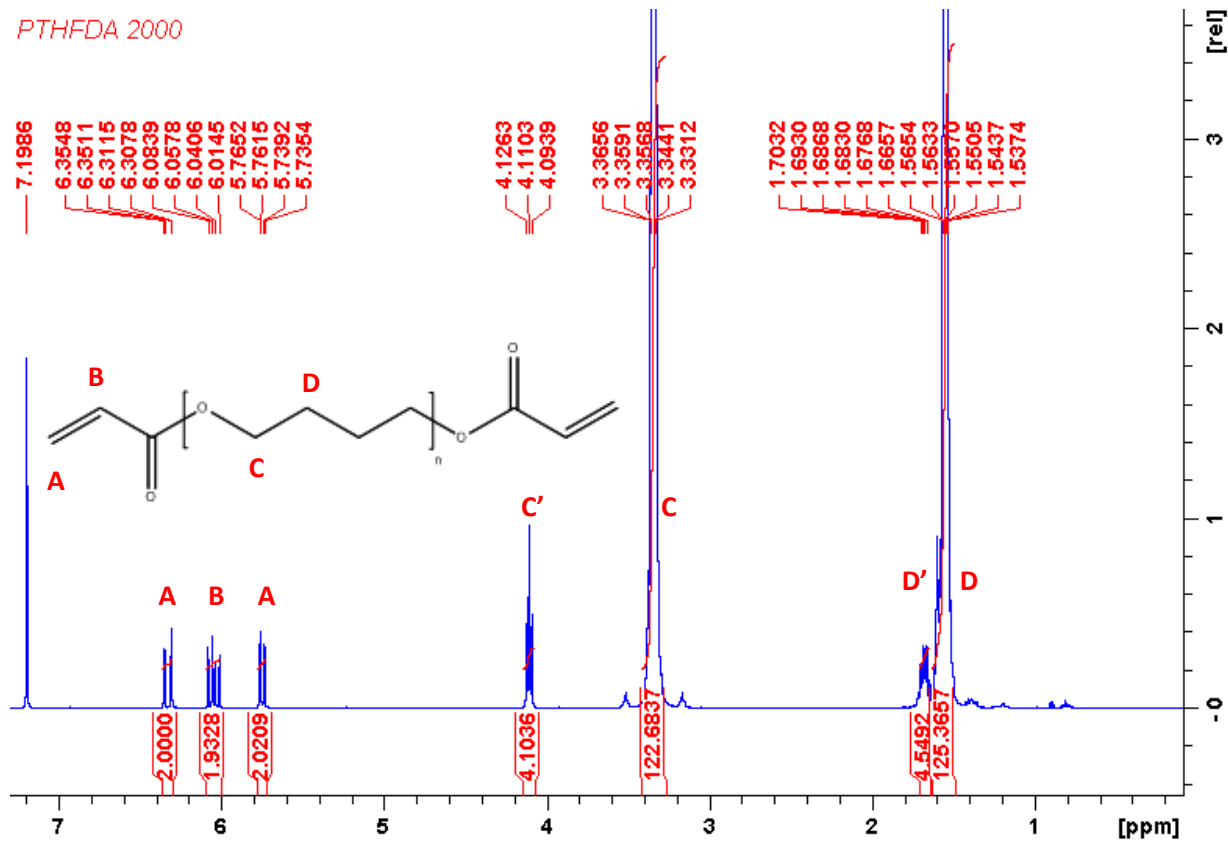


Figure S8C. ¹H NMR for PTHF₂₀₀₀DA with labeled protons. (CDCl₃, 400 MHz). δ 1.53 (m, 125H, H_D), 1.66 (m, 4H, H_{B'}), 3.34 (m, 123H, H_C), 4.11 (t, 4H, H_{C'}), 5.74 (dd, 2H, H_A), 6.04 (dd, 2H, H_B), 6.35 (dd, 2H, H_A). There are about 256 aliphatic protons, which corresponds to 32 repeat units. Each repeat unit has a mass of 72 g/mol. With the acrylate groups, total molecular mass is estimated at 2430 g/mol.

- (1) Meziane, R.; Bonnet, J. P.; Courty, M.; Djellab, K.; Armand, M. Single-Ion Polymer Electrolytes Based on a Delocalized Polyanion for Lithium Batteries. In *Electrochimica Acta*; 2011; Vol. 57, pp 14–19.
- (2) Merrill, L. C.; Ford, H. O.; Schaefer, J. L. Application of Single-Ion Conducting Gel Polymer Electrolytes in Magnesium Batteries. *ACS Appl. Energy Mater.* **2019**, 2 (9), 6355–6363.

- (3) Elmore, C. T.; Seidler, M. E.; Ford, H. O.; Merrill, L. C.; Upadhyay, S. P.; Schneider, W. F.; Schaefer, J. L. Ion Transport in Solvent-Free, Crosslinked, Single-Ion Conducting Polymer Electrolytes for Post-Lithium Ion Batteries. *Batteries* **2018**, *4* (2), 28.
- (4) Ford, H. O.; Merrill, L. C.; He, P.; Upadhyay, S. P.; Schaefer, J. L. Cross-Linked Ionomer Gel Separators for Polysulfide Shuttle Mitigation in Magnesium-Sulfur Batteries: Elucidation of Structure-Property Relationships. *Macromolecules* **2018**.
- (5) Rojas, A. A.; Inceoglu, S.; Mackay, N. G.; Thelen, J. L.; Devaux, D.; Stone, G. M.; Balsara, N. P. Effect of Lithium-Ion Concentration on Morphology and Ion Transport in Single-Ion-Conducting Block Copolymer Electrolytes. *Macromolecules* **2015**, *48* (18), 6589–6595.
- (6) Meziane, R.; Bonnet, J. P.; Courty, M.; Djellab, K.; Armand, M. Single-Ion Polymer Electrolytes Based on a Delocalized Polyanion for Lithium Batteries. In *Electrochimica Acta*; 2011; Vol. 57, pp 14–19.
- (7) Ford, H. O.; Merrill, L. C.; He, P.; Upadhyay, S. P.; Schaefer, J. L. Cross-Linked Ionomer Gel Separators for Polysulfide Shuttle Mitigation in Magnesium-Sulfur Batteries: Elucidation of Structure-Property Relationships. *Macromolecules* **2018**, *51* (21), 8629–8636.
- (8) Evans, J.; Vincent, C. A.; Bruce, P. G. Electrochemical Measurement of Transference Numbers in Polymer Electrolytes. *Polymer (Guildf)*. **1987**, *28* (13), 2324–2328.
- (9) Zhang, H.; Li, C.; Piszcza, M.; Coya, E.; Rojo, T.; Rodriguez-Martinez, L. M.; Armand, M.; Zhou, Z. Single Lithium-Ion Conducting Solid Polymer Electrolytes: Advances and Perspectives. *Chemical Society Reviews*. 2017, pp 797–815.
- (10) Diederichsen, K. M.; McShane, E. J.; McCloskey, B. D. Promising Routes to a High Li⁺ Transference Number Electrolyte for Lithium Ion Batteries. *ACS Energy Lett.* **2017**, *2* (11), 2563–2575.

- (11) Iermakova, D. I.; Dugas, R.; Palacín, M. R.; Ponrouch, A. On the Comparative Stability of Li and Na Metal Anode Interfaces in Conventional Alkyl Carbonate Electrolytes. *J. Electrochem. Soc.* **2015**.
- (12) Wu, M.; Wen, Z.; Liu, Y.; Wang, X.; Huang, L. Electrochemical Behaviors of a Li₃N Modified Li Metal Electrode in Secondary Lithium Batteries. *J. Power Sources* **2011**.
- (13) Bron, P.; Roling, B.; Dehnen, S. Impedance Characterization Reveals Mixed Conducting Interphases between Sulfidic Superionic Conductors and Lithium Metal Electrodes. *J. Power Sources* **2017**.